An adaptable microreactor to investigate the influence of interfaces on biofilm development of Pseudomonas aeruginosa

Ye zhang[1], Dina Silva[2], Daniela Traini[2], Paul Yound[1], Shaokoon Cheng[1], and Huixin Ong[3]

[1]Macquarie University
[2]Woolcock Institute of Medical Research
[3]The University of Sydney Faculty of Medicine and Health

June 7, 2021

Abstract

Biofilms are ubiquitous and notoriously difficult to eradicate and control, complicating human infections, industrial and agricultural biofouling. Current biofilm studies are commonly performed with the biofilm cultured on mono-interface and generally have neglected to consider more realistic biofilm, where diverse interfaces are involved. In our study, a reusable dual-chamber microreactor with interchangeable membranes was developed to establish multiple interfaces for biofilm culture and test. Protocol for culturing Pseudomonas aeruginosa (PAO1) on the air-liquid interface (ALI) and liquid-liquid interface (LLI) under static environmental conditions for 48h was optimized using this novel device. This study shows that LLI model biofilms are more susceptible to physical disruption compared to ALI model biofilm. SEM images revealed a unique 'mushroom-shaped' microcolonies morphological feature, which is more distinct on ALI biofilms than LLI. Furthermore, the study showed that ALI and LLI biofilms produced a similar amount of extracellular polymeric substances (EPS). As differences in biofilm structure and properties may lead to different outcomes when using the same eradication approaches, the antimicrobial effect of an antibiotic, Ciprofloxacin (CIP), was chosen to test the susceptibility of 48h-old ALI and LLI biofilms. Our results show that the minimum eradication concentration (MBCE) of CIP using our dual-chamber device reached 1600μg/ml, which is significantly higher than the conventional microtiter plate method (64μg/ml). The results highlight the importance of having a model that can closely mimic in-vivo conditions to develop more effective biofilm management strategies.

An adaptable microreactor to investigate the influence of interfaces on *Pseudomonas aeruginosa* biofilms

Zhang Ye[1,2], Dina M. Silva[2], Paul Young, [2,5], Daniela Traini[2,3], Shaokoon Cheng*[2], Hui Xin Ong*[2,4]

[1] School of Mechanical Engineering, Macquarie University, Sydney, NSW, Australia

[2] Woolcock Institute of Medical Research, Sydney, Australia.

[3] Department of Biomedical Science, Faculty of Medicine, Health and Human Sciences, Macquarie University, Sydney, NSW, Australia

[4] Faculty of Medicine and Health, The University of Sydney, Sydney, Australia

[5] Department of Marketing, Macquarie Business School, Macquarie University, Sydney, NSW, Australia

* Corresponding authors:

Shaokoon Cheng - School of Mechanical Engineering, Macquarie University, 44 Waterloo Rd., Macquarie Park, Sydney, NSW, 2113, Australia

Email: shaokoon.cheng@mq.edu.au

Hui Xin Ong - Woolcock Institute of Medical Research & Faculty of Medicine and Health, The University of Sydney, Sydney, NSW, 2037, Australia

Email: ong.hui@sydney.edu.au

ABSTRACT

Biofilms are ubiquitous and notoriously difficult to eradicate and control, complicating human infections, industrial and agricultural biofouling. Current biofilm studies are commonly performed with the biofilm cultured on mono-interfaces and generally have neglected to consider more realistic models or approaches, where diverse interfaces are involved. In our study, a reusable dual-chamber microreactor with interchangeable membranes was developed to establish multiple interfaces for biofilm culture and test. Protocol for culturing *Pseudomonas aeruginosa* (PAO1) on the air-liquid interface (ALI) and liquid-liquid interface (LLI) under static environmental conditions for 48h was optimized using this novel device. This study shows that LLI model biofilms are more susceptible to physical disruption compared to ALI model biofilm. SEM images revealed a unique 'mushroom-shaped' microcolonies morphological feature, which is more distinct on ALI biofilms than LLI. Furthermore, the study showed that ALI and LLI biofilms produced a similar amount of extracellular polymeric substances (EPS). As differences in biofilm structure and properties may lead to different outcomes when using the same eradication approaches, the antimicrobial effect of an antibiotic, Ciprofloxacin (CIP), was chosen to test the susceptibility of 48h-old *P. aeruginosa* biofilms grown on ALI and LLI. Our results show that the minimum eradication concentration (MBCE) of CIP using our dual-chamber device reached 1600µg/ml, which is significantly higher than the conventional microtiter plate method (64µg/ml). The results highlight the importance of having a model that can closely mimic *in-vivo* conditions to develop more effective biofilm management strategies.

Introduction

Biofilms are the dominant surviving model of bacteria that exist on earth [1]. It plays a crucial part in the ecosystem, either beneficial or detrimental depending on the microbial species and their growth. For example, crops can benefit from non-pathogenic biofilm growth-promoting rhizobacteria (PGPR) biofilm [2] but can also trigger foodborne illnesses in plant diseases caused by pathogenic microbial biofilms [3]. Also, while biofilms can help degrade pollutants in liquid and gaseous effluents in wastewater treatment plants [4], undesired biofilm formation in drinking water, oil pipelines, and ship hulls can lead to biofouling and biocorrosion, which undermine operation safety and loss of productivity [4]. Furthermore, biofilms are typically associated with clinical chronic, nosocomial, and medical device-related infections [5-8].

The formation of biofilm starts with planktonic bacteria adhering to the surface and encasing the proliferated colonies in self-produced extracellular plyometric substance and become matured biofilm [1]. Biofilms protect the microorganism from hostile physical and chemical environments such as altered pH, osmolarity, nutrients scarcity, mechanical and shear forces, and block bacterial biofilm communities' access from antibiotics and host's immune cells [9]. Their properties are determined by both inherent biological attributes of bacterial strains and external environmental factors. Among all the environmental factors, surfaces play a critical role since their properties directly affect bacteria's initial attachment, biofilm maturation, and final detaching. Studies on the impact of surface roughness, charge, hydrophobicity, tension, wettability, and microtopography on biofilm growth [10, 11] have persistently modeled biofilm as solid-attached structures submerged in liquid. Other studies have explored the development of biofilm aggregates cultured in agarose have been used to mimic the intrinsic properties of human tissue in various fields [12, 13], such as wound microenvironment. However, the variations in terms of interface type have been neglected. Furthermore, antibiotics have been widely used to treat biofilm infection diseases with multiple delivery paths, including parenteral, enteral, transdermal, inhalation, oral, and topical. The interaction between antibiotics and biofilms also varies depending on interfaces. A greater understanding of the influence of interfaces on biofilms will help to develop more efficient and targeted eradication approaches.

2

For this purpose, we proposed a dual-chamber microreactor with interchangeable interfaces to study biofilm structure and susceptibility to drugs. Our model brings the advantages of a microfluidic device, which include reduced sample volume and reagent consumption and precise environmental control. Moreover, the curing approach and reversible bonding technique adopted for device fabrication and assembling, further helps to reduce experimental time and cost and brings greater flexibility for sample manipulation. Compared with conventional antimicrobial susceptibly testing methods, our device can be considered more physiobiologically relevant in mimicking the microenvironment that biofilm grows and interacts with antibiotics.

Pseudomonas aeruginosa is a ubiquitous pathogen that could colonize multiple environments and establish a biofilm within 24 h [14]. It can cause a variety of infections, such as chronic lung infection [15] and urinary tract infections (UTIs) [16], and its accentuated antibiotic resistance during biofilm growth poses a significant threat to the medical community. The biofilm developed in the respiratory system can be modeled as biofilm formed on the air-liquid interface (ALI), while biofilm developed in the urinary tract can be best characterized by liquid-liquid interface (LLI) model biofilm. In this study, we used this novel device to optimize a protocol for culturing*Pseudomonas aeruginosa* (PAO1) on ALI and LLI, respectively, under static environmental conditions for 48h. Biofilm susceptibility was also evaluated after exposure to ciprofloxacin from the substrate side to mimic systemic circulation exposure, which permeates through a physical barrier to reach the biofilm site.

Materials and Methods

Materials

Polydimethylsiloxane monomer and curing agent (Sylgard 184, Dow Corning) were purchased from Revolution Industrial (Australia). Formlab® Clear resin V4 was obtained from Core Electronics (Australia). Isopropyl alcohol (IPA) ([?]99%) and ethanol (80% v/v) were obtained from Chem-supply Pty Ltd (Australia). Ambersil(r) polymer remover was purchase from RS components Pty Ltd (Australia). Hydrophilic porous polyester (PETE) membrane (pore size 0.2µm, pore density 3 x 108 (pores/cm^2), open area 9.4%, thickness 10µm, bubble point 20psi, water flow rate 10mL/min/cm^2, airflow rate 3L/min/cm^2) was purchased from Sterlitech (USA). Translucent silicon rubber (TRANSIL®) was obtained from Barnes Products Pty Ltd (Australia). Tygon tubing (1.59mm OD x 0.51mm ID), 23G stainless steel couplers (0.63mm OD x 0.33mm ID), and razor-sharp stainless-steel biopsy punches (0.5mm and 1.25mm OD) were purchased from Darwin Microfluidics (France). Stainless steel screws and nuts were obtained from Small Parts & Bearings (Australia). Blunt needles (22G) and sterile disposable syringes were obtained from Livingstone (Australia). *Pseudomonas aeruginosa* (PAO1 ATCC 15692) was purchased from the American Type Culture Collection (ATCC, Rockville, USA). Cation-adjusted Mueller-Hinton Broth (CAMHB) was purchased from BD Biosciences (Australia). Phosphate-buffered saline (PBS), LB Broth with agar (Lennox), Alcian blue (1% w/v in acetic acid, 3% v/v pH 2.5), AeraSeal® Film, and formaldehyde solution ([?]36.0% in water) were purchased from Sigma Aldrich (Australia). FilmTracer LIVE/DEAD(r) Biofilm viability kit was obtained from Thermo Fisher Scientific (Australia). Ciprofloxacin hydrochloride was supplied by MP (Biomedical Australasia Pty Limited, Australia). Milli-Q water was obtained from Biopak(r) Polisher system (Merck KGaA, Germany).

Device design and fabrication

The microreactor (Fig.1) consists of a dual-chamber design (basal and apical) physically separated by a porous hydrophilic PETE membrane, used as the substrate for biofilm growth. Each device comprised three identical dual-chamber flow cells allowing for the testing of multiple experimental setups in parallel. The dimensions of the chamber were: 1mm (width) x 4mm (length) x 0.5mm (height). The flow chambers (Fig. 1-B) were fabricated using PDMS by 3D printing microfluidic fabrication technique [17]. The molds for PDMS casting were printed using a clear resin on a Form2 3D printer (Formlabs), washed for 15 min with IPA (Formlabs, Form wash), and cured under UV light for 90 mins at 65degC (Formlabs, Formcure). Before pouring the PDMS, the mold was spray-coated with polymer remover to protect the mold surface and to assist with the PDMS removal after the curing process. PDMS monomer and curing agent were mixed (10:1 w/w), cast into the mold, degassed, and cured at 65degC for 12h. After cooling, the PDMS chamber was

peeled off from the mold, and the inlet and outlet holes were punched using a 0.5mm biopsy puncher. Two pieces of thin silicon gaskets (0.3mm) were placed between the membrane and the PDMS layers to prevent leakage and protect the membrane from the mechanical bounding force. The silicone gaskets (Fig. 1-C) were fabricated by pouring silicone on the plastic sheet and pressing the 3D printed template into the uncured silicone mix and against the plastic sheet. The silicone gaskets were cured at room temperate for 25min and then peeled from the plastic sheet.

Device assembly

Reversible mechanical bonding of the multiple layers (Fig. 1-A) was obtained using two pieces of acrylic Plexiglas covers (76mm x 25 mm x 3mm) with holes aligned with the position of the inlet, outlet and bonding holes in the PDMS layers. The mechanical bonding was achieved by twelve screws and nuts positioned around the perimeter of the flow chamber to ensure the alignment of the layers and the interface area between the two chambers. The flow into the channels was supplied through microbore tubing connected to stainless-steel couplers (23G), inserted into the inlet and outlet ports. Before the bacteria inoculation, 1 mL sterilized water was injected into two chambers to ensure no leaking occurs.
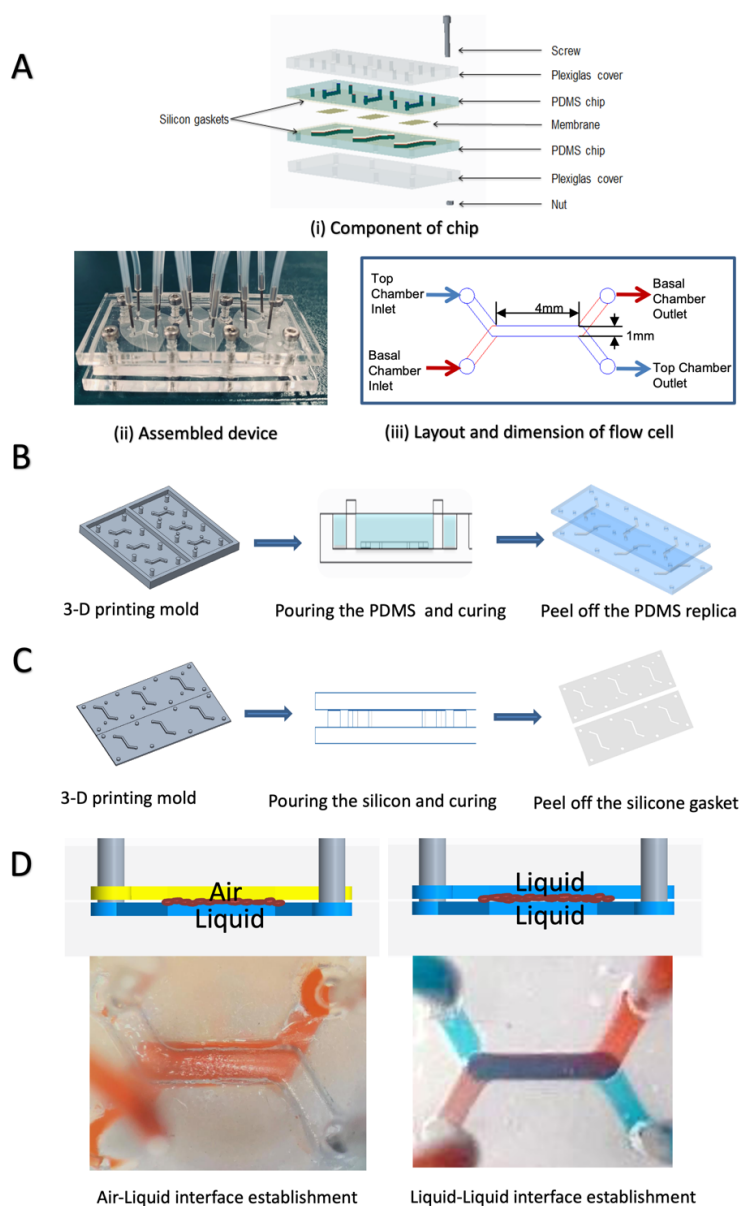
Figure 1: Dual-chamber microfluidic device fabrication and assembly. A) Components of chip and assembled device. B) PDMS chips fabrication process. C) Silicon gaskets fabrication process. D) Interface establishment - ALI was established when the bottom chamber was filled with liquid and the top chamber was filled with air while the LLI was created when both chambers were filled with liquid.

Figure 1 : Dual-chamber microreactor fabrication and assembly. A) Components of chip and assembled device. B) PDMS chips fabrication process. C) Silicon gaskets fabrication process. D) Interface establishment - ALI was established when the bottom chamber was filled with liquid and the top chamber was filled with air, while the LLI was created when both chambers were filled with liquid.

Device sterilization

Before inoculation, the PDMS chips, acrylic Plexiglas covers, and silicon gaskets were sonicated with Milli-Q water for 480s, rinsed with an ethanol solution (80% v/v), and exposed to UV light for sterilization for 30 min. The PETE membranes and tubing were sterilized using the autoclave (121°C/ 20min). All the

components were assembled aseptically in the biosafety cabinet.

Device inoculation and biofilm formation

P. aeruginosa from frozen stocks was grown on agar plates for 16-18h at 37°C. To prepare liquid pre-culture, one colony was transferred into 1mL of CAMHB media (3g/L beef extract, 17.5g/L casein hydrolysate, 1.5g/L starch, pH 7.0), incubated for 16-18h at 37°C, and shaken at 200 revolutions per minute (RPM). The overnight pre-culture was diluted 1:30 v/v in fresh media, incubated for 2h at 37°C, and shaken at 200 RPM. The inoculum size was optimized by testing two different standardized densities, which are OD_{600} = 0.04 and 0.4, respectively, to obtain a fully covered membrane within 48 h of growth. Before inoculation, the inoculum size controls were also obtained by viable colony forming units (CFU) counts.

For the device inoculation, 100μl of CAMHB media was injected into the basal chamber through the basal chamber inlet before 100μl of bacterial inoculum was injected into the top chamber through the top channel inlet. After inoculation, the excess media and inoculum were discarded by the tubing removal, and the chip was sealed with a sterile and breathable film (AeraSealTM) and incubated at 37°C for 2h under static conditions to allow bacteria attachment. Two different interface models were tested – ALI and LLI. For the ALI establishment, the culture media was removed from the apical chamber after 2h of bacterial adhesion. For LLI conditions, the apical media was removed after 2h of attachment and replaced by fresh culture media in the apical chamber. Biofilms were grown at 37°C for 48h, and the media on the basal chamber was refreshed after 24h of culture.

Device repeatability test

The repeatability of this microreactor was evaluated by quantifying biofilm growth under ALI and LLI models, using CFU counts. Three biological replicates were performed for biofilm formation on ALI and LLI. Two devices containing six flow cells were inoculated for each test model, and another device infused with media was used as controls. Controls for inoculum size were performed after each inoculation by viable colony counts to ensure that differences in the inoculum size were minimal. After 48h, each membrane was aseptically removed from the device, gently dip-washed in 1mL of sterile PBS, and subsequently transferred to a tube containing 1 mL of sterile PBS. To disrupt the biofilm, the membranes were sonicated for 280s at 47kHz and 1.8W/cm2, previously shown to cause no deleterious effect on the colony-forming ability of P. aeruginosa [18]. Following the disruption, ten-fold serial dilutions of the detached bacterial suspensions were performed in sterile PBS, plated on LB agar plates, and incubated at 37 for 16-18h. Viable colony counts were calculated using equation 1:

$$\frac{CFU}{mL} = \frac{N \times 10}{10^{-D}} \quad Eq. (1)$$

where N represents the colony number and D represents the number of 1:10 dilutions. Six randomly selected membranes were analyzed by scanning electron microscopy (SEM) to confirm that bacteria had been removed from the surface.

Scanning Electron Microscopy (SEM)

The morphology of the biofilms grown on the devices was visualized using scanning electron microscopy (SEM, JEOL, JMC-6000 NeoScopeTM Benchtop SEM, USA) at 15kV. The devices were disassembled, and membranes gently dip-washed in sterilized water before fixation in a formaldehyde solution in PBS (4% v/v) for 90min. After fixation, membranes were gently rinsed with water and air-dried at room temperature. Before imaging, the membranes were sputter-coated with gold for 2min using a Smart Coater (JEOL, USA). At least three membranes from each experimental condition were analyzed.

Confocal laser scanning microscopy (CLSM)

The biofilm formed on different interfaces was investigated using FilmTracer LIVE/DEAD(r) Biofilm viability kit according to the manufacturer's specifications. The samples were gently washed with sterilized water followed by staining with LIVE/DEAD solution for 25mins at 37degC in the dark. Excess dye was removed using sterilized water. The biofilms were then fixed for 40 min by infusing PFA solution (4% v/v in PBS).

The sample was rinsed with sterile water and mounted on a glass slide. Fluorescence was observed using a confocal laser scanning microscope (Olympus FluoView, inverted FV 3000RS IX83, 100x magnification oil immersion objective). The image was acquired using 488 nm and 660nm incident light. The z-stack images were taken with a step of 1µm, and the resolution was 1,024×1,024 pixels. All experiments were performed in duplicate. 3D reconstruction view and 3D z-stack projection images were obtained, and fluorescence intensity measured using ImageJ. The ratio of live cells to dead cells was compared using the fluorescent intensity ratio of green to red in 3-D projected z-stack CLSM images to quantify the difference between biofilm formed on different interfaces. For analysis, the images were obtained from two replicates which three images pick on each replicate. Thus, six images in total for each biofilm model were collected for statistical analysis.

Extracellular polymeric substances (EPS) staining

Alcian blue staining was used as a colourimetric-based approach to detect the polysaccharides in the extracellular polymeric substances [19]. The membrane was aseptically removed from the device, gently washed with sterilized water, and then fixed using 4% (v/v) formaldehyde solution in PBS for 40min. The membrane was rinsed with water again and then immersed in Alcian blue (1% w/v in acetic acid, 3% v/v pH 2.5) for 15mins. Excess dye was removed by multiple rinses with water. Images were obtained using NanoZoomer-SQ Digital slide scanner C13140-01 (Hamamatsu). Eight images were collected at 40x magnification from each sample, and the mean red, green and blue (RGB) ratio of Alcian blue and standard deviation were obtained using ImageJ.

Antibiotic Treatment Test

Ciprofloxacin (CIP) is a broad-spectrum antibiotic that is effective against PAO1[20] and hence has been used as the model antibiotic in this study. To assess the effects of the different interface on *P. aeruginosa* susceptibility to CIP, the 48h-old biofilms were exposed to a range of concentrations (50-1600µg/mL) for 6h. For the antibiotic treatments, a stock solution of CIP was prepared in water, and working solutions were freshly prepared by dilution of the stock in culture media. The antibiotic solution was injected into the basal chamber, and the biofilm interacts with antibiotics from the substrate side for 6h at 37°C. The susceptibility was assessed by CFU counts according to the procedure described in section 2.6.

Statistical Analysis

The repeatability of culturing biofilms at different interfaces was examined by calculating the standard deviations across all experiments. All data are expressed as Log (CFU/mL). Unpaired t-tests were performed to determine the significant differences between the biofilm formed at ALI and LLI. The antibiotic susceptibility of biofilm formed on ALI and LLI was investigated using one-way ANOVA. Graphs show means and error bars indicate the standard error of the mean. All the statistical analysis was performed using Graphpad Prism 7.0.

Results and Discussion

An adaptable dual-chamber microreactor has been developed incorporating different interfaces and surfaces to investigate the effects on biofilm development in terms of morphological properties, colony counts, and responses to antibiotics. Compared to conventional mono-interface reactors, the dual-chamber device offers significant advantages in mimicking the relevant physiologic and environmental settings in which bacteria thrive, offering the potential for more targeted experiments to deliver precise outcomes.

Device fabrication and assembly

The fabrication process of PDMS chips using 3D printing illustrated in Fig. 1-C, shows the versatility of the microfluidic system with affordable equipment and straightforward protocols [21]. PDMS is the ideal material for the fabrication of microfluidic devices having great biocompatibility, chemical stability, gas permeability, transparency, low cost and ease of molding [22]. The intermediary gaskets (Fig. 1-D) fabricated with silicone (a non-toxic, inert, and soft material) were introduced to cushion the mechanical force created by the screw and nuts and to prevent leakage from the flow cell. The assembled dual-chamber device comprises six layers

7

(Fig. 1-A), with two acrylic Plexiglas cover layers, two PDMS layers containing the flow chamber, and middle layers of gaskets. The acrylic Plexiglas covers help distribute the bonding force evenly on the PDMS chips to seal the system. Several bonding techniques have been used in microfluidic devices such as surface plasma and corona discharge that permanently bond PDMS layers with glass or other PDMS layers [23]. However, these techniques require specialized equipment. Moreover, several end-point sample analysis methods require the device to be disassembled, which could potentially disrupt the biofilm matrix, and consequently, the use of an irreversibly bonded device is limited. For analysis that requires many replicates, using permanently bonded devices could also be both costly and time inefficient. Therefore, the reversible mechanical bonding developed in our device will offer more flexibility and convenience for endpoint sample manipulation. The ability to fit different membranes in the same device enables the testing of different surfaces, and the device can be reused after sterilisation to reduce the cost and time of production. The establishment of the ALI and LLI methods is illustrated in Fig.1-D using red and blue dyes. The ALI method was established when the bottom chamber was filled with liquid and the top chamber filled with air, while the LLI was created when both chambers were filled with liquid.

Optimization of inoculum concentration and biofilm attachment time

Inoculum size optimization was performed to establish the formation of a mature biofilm throughout the membrane in 48h. The investigated inoculum density was standardized to OD_{600}=0.04 and OD_{600}=0.4 with inoculation times of 2h and 24h. Fig. 2 presents the microphotographs of the biofilms grown from different inoculum densities and with different attachment periods. Biofilms from low-density inoculum (OD_{600}=0.04) with 2h attachment time were scattered throughout the membrane, while biofilms from the same density with attachment time of 24h, completely covered the membranes. Biofilms grown from high-density inoculum (OD_{600}=0.4) formed a homogeneous layer on the membranes after 2h of attachment. This condition was chosen as the optimal parameter to carry out the experiments throughout this study.
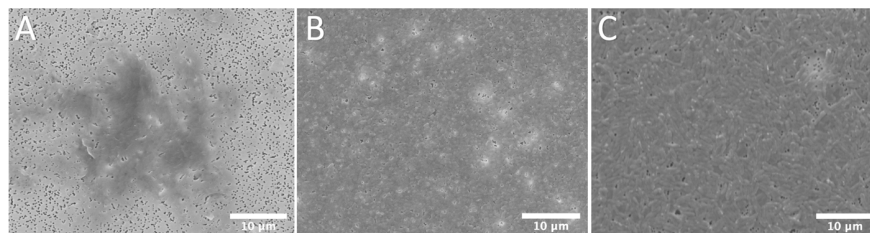
Figure 2: SEM imaging of bacteria attachment using different concentration of inoculum. A) inoculum size: OD_{600}=0.04; attachment time: 2h. B) inoculum size: OD_{600}=0.04; attachment time: 24h. C) inoculum size: OD_{600}=0.4; attachment time: 2h.

Figure 2 : SEM imaging of bacteria attachment using different concentration of inoculum. A) inoculum size: OD_{600}=0.04; attachment time: 2h. B) inoculum size: OD_{600}=0.04; attachment time: 24h. C) inoculum size: OD_{600}=0.4; attachment time: 2h.

Device performance repeatability for biofilm culture

The device performance was further confirmed by testing its repeatability on the formation of 48h-old biofilms over a determined number of experiments. Three rounds of experiments were performed (biological triplicates), and each round contains six technical replicates. A total of eighteen replicates for each biofilm model (ALI and LLI) were obtained. The inoculum solutions were standardized at $OD_{600} = 0.42 \pm 0.03$ (mean $\pm$ SD), which corresponds to Log (CFU/mL) = 8.58 $\pm$ 0.14 (mean $\pm$ SD). After 48h of growth, the number of attached cells (biofilm) and the number of detached cells washed off from the membrane after rinsing was obtained by viable colony counts. Results expressed as Log (CFU/mL) and statistical analysis are presented in Table 1 for the ALI and LLI systems. The standard deviation (SD) for detached, attached,

8

and total biofilm cultured on ALI was 0.99, 0.87 and 0.97 log CFU/mL, respectively, and was 0.98, 0.95 and 0.91 for LLI, respectively. To our knowledge, no comparable data is available since other microdevices are unable of collecting CFU numbers due to the constrain related to the nature of other devices that cannot be disassembled without damaging the cells.

Table 1. Summary statistics of the number of sessile cells recovered from membranes after biofilm formation on ALI and LLI model surfaces.

	ALI	**ALI**	**ALI**	**LLI**	**LLI**	**LLI**
	Deatched	**Attached**	**Total**	**Deatched**	**Attached**	**Total**
Mean	6.06	7.19	7.24	6.23	6.94	7.15
SD	0.99	0.87	0.87	0.98	0.95	0.91
SEM	0.24	0.20	0.20	0.23	0.22	0.22

Detached = cells washed off by rinsing; attached = cells remaining on the membrane after rinsing and detatched from the membrane after sonication; total = the sum of detached and attached. The mean value, standard deviation (SD) and standard error of the mean results (SEM) are expressed as Log(CFU/mL) of N=18.

Characterization of biofilms grown under ALI and LLI

Resistance to physical disruption, such as mechanical or hydrodynamic shear strength, is one of the most critical characteristics to be considered when investigating biofilm eradication strategies. In this study, the differences between the biofilms formed on different interfaces (ALI and LLI) was compared by assessing the CFU number of detached, attached and total biofilm collected from eighteen replicates. Fig. 3 shows the total CFU (left) and the ratio of the attached to the total (right) is compared.
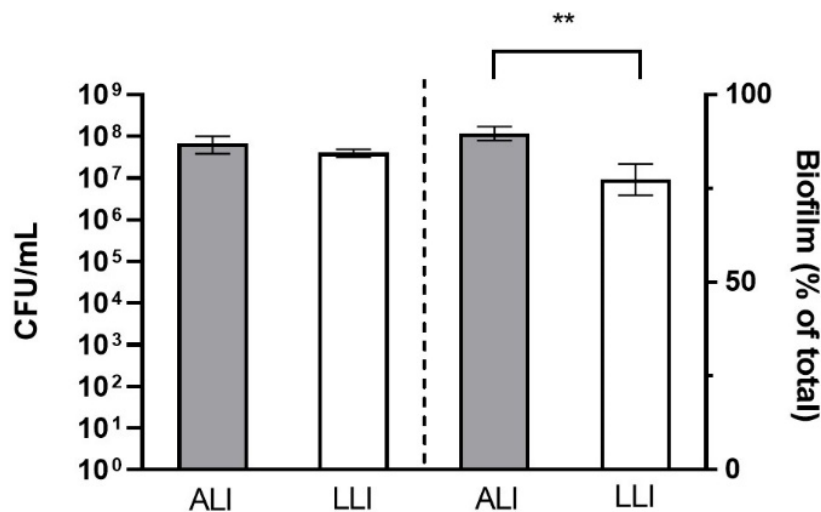
Figure. 3: Comparison of biofilm formed at ALI () and LLI () assessed by CFU/mL and the percentage of the attached to the total. (n=18, mean $\pm$ SEM) ** $p<0.01$ (using unpaired t-tests).

No significant differences were observed between the biofilms grown on ALI and LLI models when comparing the total CFU number. However, when comparing the proportion of attached bacteria relative to the total (attached + detached), a significantly higher proportion of biofilm formation was observed for biofilms

9

growing on ALI than LLI. While the overall volume of biofilm in ALI and LLI were similar, biofilms grown on ALI are more resilient and more difficult to detach from the membrane. Conversely, biofilms grown on LLI are more vulnerable. Hence the percentage of detached bacteria is greater. Also, the variability for biofilms grown on LLI is wider, suggesting that these biofilms are more heterogeneous.

Biofilms can adapt their architecture to cope with different hydrodynamic conditions and nutrient availability [24]. The interface on which the biofilm grows specifically determines the availability and permeability of nutrients and thus will have an impact on the morphology and properties of the biofilm. Several studies have attempted to investigate the properties of biofilm formed on a particular interface. Wu et al. [25] conducted interfacial rheological measurements on ALI biofilms produced by *Escherichia coli* and found that hydrophobic curli fibres associated with the bacteria improve strength, viscoelasticity, and resistance to ALI biofilms. Another study by Rühsa *et. at.* [26] measured the transient elasticity and viscosity of the biofilm formed at the water-oil interface using interfacial rheology and pendant drop tensiometry and found that the ability to form biofilms against oil improved with increasing hydrophobicity. However, these studies are unable to provide comparative studies on the effect of the interface type using a single platform to control the variables, as most of the instruments are designed to investigate only one specific interface.

While microfluidic instruments have been developed to examine the effect of external forces such as the hydrodynamic shear force on the growth of biofilm [27], most of these devices are irreversibly bonded, which severely undermine the flexibility and potential of incorporating other end-point analysis approaches such as the approaches we adopted in our study. The dual-chamber microreactor presented in this study overcome these challenges by having a design that can be disassembled and with the capabilities to incorporate multiple interfaces with interchangeable membrane while keeping other variables (e.g., dynamic flow conditions) constant between experiments.

The morphology of 48h-old ALI and LLI PAO1 biofilms were also visualized using CLSM and SEM (Fig.4). The 3D reconstruction of z-stack CLSM images (Fig. 4 A and D) show that a layer of biofilm was formed over the membrane and the thickness of the biofilm was approximately 5μm (Fig. 4 B and E). Mushroom-shaped bacterial aggregates dispersed across the membrane were observed in SEM images in both ALI and LLI models for PAO1 biofilms (Fig. 4 C and F), and their shapes are more distinct in the ALI compared to the LLI. This is in good agreement with Moller, S., et al. [5] which demonstrated that biofilms grown under nutrient depletion are highly structured, and the 'mushroom-shaped' microcolonies are interspersed between open water channels. In our study, biofilms have been grown in static conditions with a finite amount of culture media supplied, resulting in nutritional exhaustion conditions towards the later stages of bacteria growth. Moreover, in comparison to ALI culture, LLI culture has more nutrients coming from the top chamber. Thus, the mushroom-shaped microcolonies showed in our SEM images in both the LLI and ALI models, and the difference between them corroborated Moller 's [5] discoveries.

Biofilms have also been known to have open water channels that facilitate the diffusion of nutrients and waste products between the external environment and biofilm and within the biofilm matrix [8]. These channels are also evident in our CLSM images (black space unstained with green and red) and SEM images (black holes in the biofilm). Comparing Fig. 4 B and E, the structure of the LLI model biofilm is more dispersed, while the ALI model biofilm is more aggregated. Also, more water channel holes can be seen in the LLI model biofilm SEM images. We hypothesize that the media transmission occurring in the LLI model is higher than the ALI model, enabling more water channels to be formed to facilitate the transport of nutrients and waste. Differences in the structure of the biofilm matrix could contribute to the differences in mechanical properties, which has been demonstrated through the scattered structures (LLI model biofilm), making it more vulnerable to disruption of physical forces. Consequently, the adhesion strength between the biofilm and the underlaid surface and the cohesive force within the biofilm is weaker for the LLI biofilm relative to the ALI biofilm. This further supports the findings in Fig. 3 that LLI biofilms are more susceptible to physical removal.
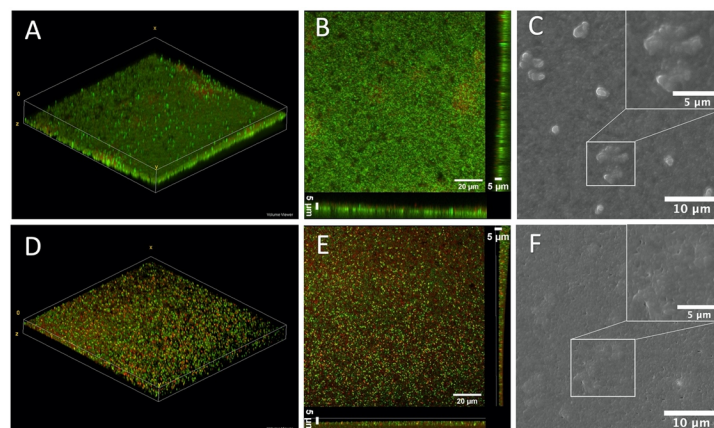
Figure 4: Morphology of biofilms grown under ALI (A-C) and LLI (D-F) interfaces: A) and D), representative 3D reconstruction of z-stack CLSM images B) and E) are 3D projected and orthoclase views of z-stacks obtained from the CLSM images. The live bacteria were stained with SYTO9 (green) and dead bacteria were stained red-fluorescent propidium iodide. C) and F) are representative SEM images of PAO1 biofilms showing the mushroom-shaped aggregates, the upper right corner is magnified 'mushroom-shape' aggregates.

Figure 4: Morphology of biofilms grown under ALI (A-C) and LLI (D-F) interfaces: A) and D), representative 3D reconstruction of z-stack CLSM images B) and E) are 3D projected and orthoclase views of z-stacks obtained from the CLSM images. The live bacteria were stained with SYTO9 (green), and dead bacteria were stained red-fluorescent propidium iodide. C) and F) are representative SEM images of PAO1 biofilms showing the mushroom-shaped aggregates, the upper right corner is magnified 'mushroom-shape' aggregates.

During biofilm formation, both live and dead bacteria are encased within the EPS matrix. The CLSM images (Fig.4) show a distinct qualitative difference between ALI and LLI biofilms in terms of the amount of live and dead cell. More specifically, biofilm grown on ALI had a higher ratio of living bacteria than the biofilm formed at LLI (Fig. 5). This result corroborates with our previous results in Fig. 3, showing that biofilms formed at LLI were more susceptible to the physical disturbance compared to ALI cultured biofilm, leaving more bacteria on the membrane for ALI model biofilm.
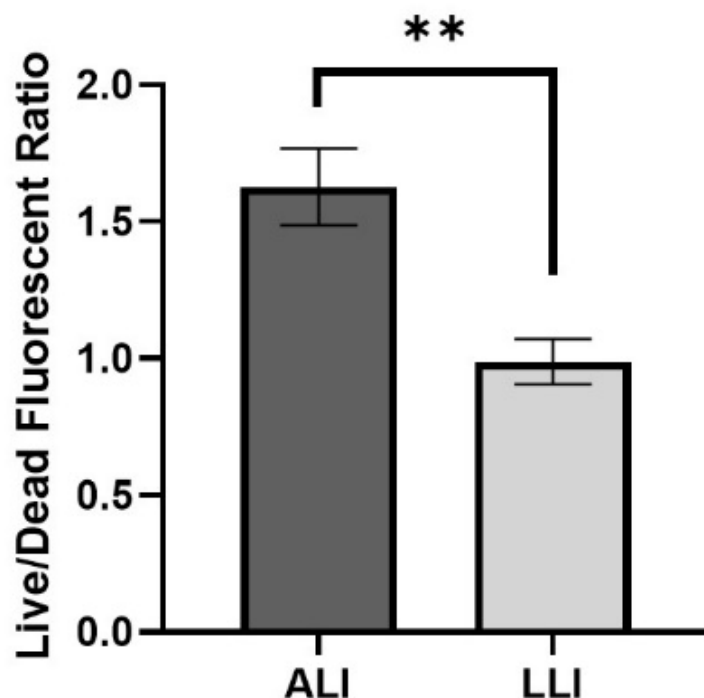
Figure 5: Comparison of the Live(green)/Dead(red) fluorescent ratio of biofilm formed on ALI and LLI models. (n=6, mean ± SEM) ** P<0.01 (using unpaired t-tests).

Extracellular polymeric substances staining

Alcian blue was used to stain polysaccharides in EPS to provide semi-quantitative data for biofilm formed on both the ALI and LLI models. The RGB ratio obtained from bright-field images of the stained biofilms is depicted in Fig.6. As the media contains starch, a relatively low blue ratio ([?]0.3) was detected in the control group (membrane only). The RGB ratio for biofilm samples is significantly higher than the control sample, indicating that the biofilm has formed on the membrane. However, no significant difference between the ALI and LLI was present, suggesting that the quantity of EPS produced by different biofilm models is similar.
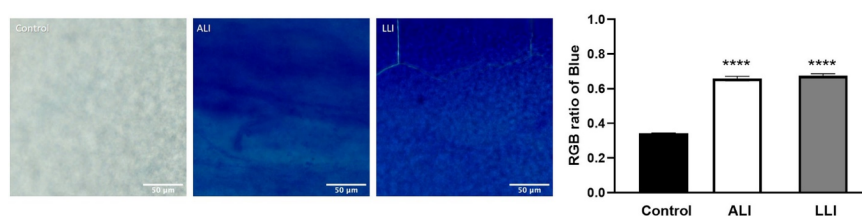

Figure 6 : Representative microscopic images of Alcian blue staining and comparison of RGB ratio of samples stained with Alcian blue. Error bars were produced from the standard deviation of six replicates. (n=8, mean ± SEM) **** P<0.0001 (using unpaired t-tests).

Antibiotic Treatment Test

12

The effect of antibiotic treatment on biofilms grown in different interfaces was evaluated to understand the differences in biofilm susceptibility and to validate our model as a more realistic screening tool in biofilm management. The results of the antibiotic susceptibility test in the range of 50-1600μg/mL for the ALI and LLI interfaces are depicted in Fig. 7. Data is presented using the number of detached, attached and total CFUs. CIP induced a concentration-dependent decrease for the biofilm, detached bacteria, and total counts for both interfaces. Statistical differences were only observed for concentrations from 800μg/mL, and biofilms were not eradicated at the highest concentration tested (1600μg/mL). This is probably due to the biofilm's complex structure and the presence of EPS, which creates an antibiotic gradient in the biofilm community [5-8].

The antibiotic effect on the biofilms was further corroborated by the SEM images (Fig. 8), showing the differences in biofilm density across the membranes when compared to the control (without antibiotic).
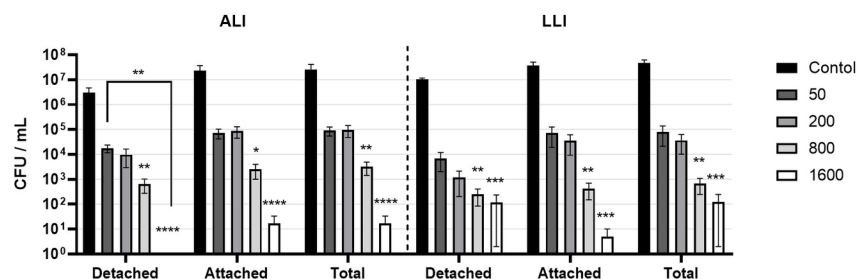
Figure 7: Comparison CFU/mL data of detached, attached and total bacteria after exposure to CIP (50, 200, 800, and 1600μg/mL) for 6h. Antibiotic exposure was performed from the basal chamber. (n=6, mean ± SEM), * $p < 0.05$; ** $p < 0.01$; *** $p < 0.001$; **** $p < 0.0001$ (using one-way ANOVA test).
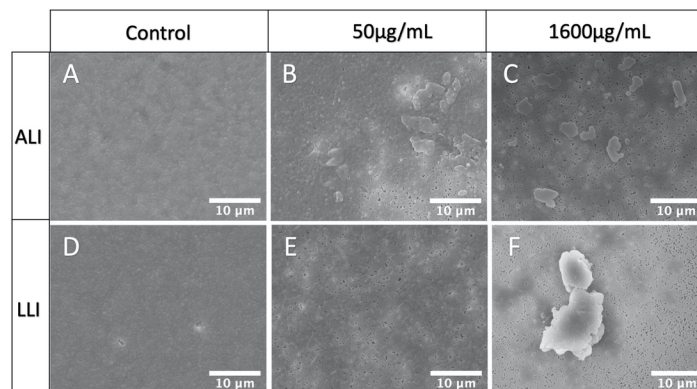
Figure 8: Representative microphotographs of 48h-old biofilms exposed to CIP for 6h: A) untreated biofilm grown in ALI; B) and C) biofilms grown in ALI and treated with 50μg/mL and 1600μg/mL of CIP, respectively; D) untreated biofilm was grown in LLI; E) and F) biofilms grown in LLI and treated with 50μg/mL and 1600μg/mL of CIP, respectively.

Conventional methods to determine antibiotic efficacy are routinely performed under the standard liquid culture condition using the broth microdilution technique, and 96-well microtiter plates [28-31] and the

standard protocol for measuring minimal inhibitory concentration (MIC), which required to inhibit growth or kill planktonic bacteria [32] and the minimal biofilm eradication concentration (MBEC) [33] were proposed. Several novel methods, such as the Calgary Biofilm Device [34] and microfluidic devices [35], were developed to improve the measurement of MBEC as well. However, the biofilms were mostly cultured by submerging in the liquid, and antibiotics can only be delivered through one approach (biofilm submerged in antibiotics). In our study, injecting the antibiotic solution into the basal chamber and interacting with biofilm from the substrate attaching side illustrates an alternative way to mimic the antimicrobial mechanism that the drug being administrated through oral or parenteral routes and taken to the biofilm site through the systemic circulation. The MBEC of 3-day PAO1 biofilm using CIP reported by Wu et. al. using the microtiter plate method was 64μg/mL [31], while our results show that significantly higher CIP concentration is needed to achieve a 50% decrease in the biofilm. The differences across models highlight the importance of having a model that can closely mimic the environmental conditions where these communities persist. Thus, recognizing the differences in biofilms thrived on various interfaces could shed light on designing more effective and efficient control methods.

Conclusions

This paper introduces a novel reusable dual-chamber microreactor to provide multiple interfaces for biofilm culture and test. The reusable assembling technique provides greater flexibility to grow biofilms and to screen the effects of different interfaces on biofilms, both quantitatively and qualitatively. Protocols for culturing biofilm on ALI and LLI in static condition and following test methods are feasible and repeatable. PAO1 biofilms grow on ALI and LLI show differences in morphology and resistance to physical interruptions. Our dual chamber device also enables efficacy testing of antibiofilm strategies in an environment that closely mimics *in vivo* biofilm growth conditions, producing more accurate test results. 48h-old PAO1 biofilms cultured on ALI and LLI show high resistance when antibiotic delivered from the substrate side.
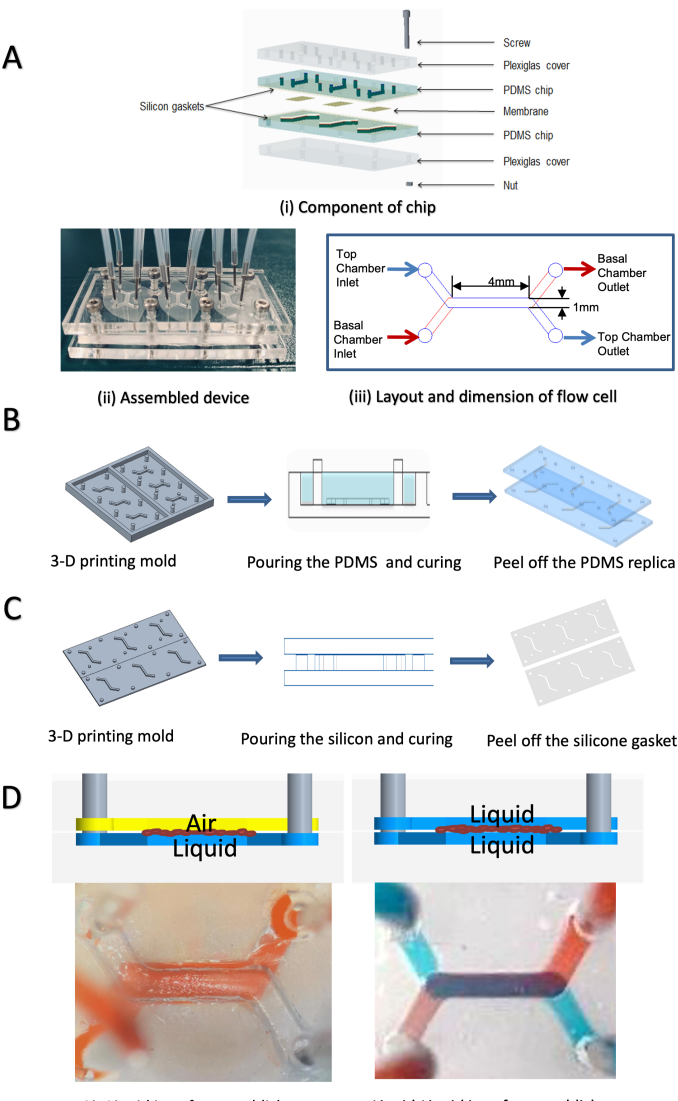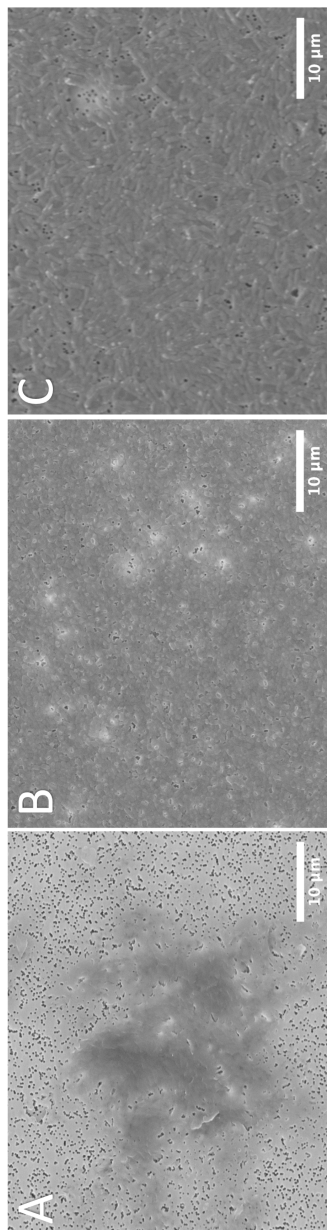
ACKNOWLEDGMENTS

REFERENCES

[1] R.M. Donlan, Biofilms: microbial life on surfaces, Emerging infectious diseases 8(9) (2002) 881-890.

[2] T. Rudrappa, Causes and consequences of plant-associated biofilms, FEMS Microbiol Ecol 64 (2008) 153-166.

[3] C. Buttimer, O. McAuliffe, R.P. Ross, C. Hill, J. O'Mahony, A. Coffey, Bacteriophages and Bacterial Plant Diseases, Front Microbiol 8 (2017) 34-34.

[4] M.H. Muhammad, A.L. Idris, X. Fan, Y. Guo, Y. Yu, X. Jin, J. Qiu, X. Guan, T. Huang, Beyond Risk: Bacterial Biofilms and Their Regulating Approaches, Frontiers in microbiology 11 (2020) 928-928.

[5] Z. Khatoon, C.D. McTiernan, E.J. Suuronen, T.-F. Mah, E.I. Alarcon, Bacterial biofilm formation on implantable devices and approaches to its treatment and prevention, Heliyon 4(12) (2018).

[6] S. Sunarintyas, Bioadhesion of Biomaterials, in: F. Mahyudin, H. Hermawan (Eds.), Biomaterials and Medical Devices: A Perspective from an Emerging Country, Springer International Publishing, Cham, 2016, pp. 103-125.

[7] K. Vickery, J. Allan, A. Jacombs, P. Valente, A. Deva, Prevention of Implantable Medical Device Failure (IMD) Associated with Biofilm Infection, AJIC: American Journal of Infection Control 39(5) (2011) E45-E45.

[8] P. Stoodley, L. Hall-Stoodley, B. Costerton, P. DeMeo, M. Shirtliff, E. Gawalt, S. Kathju, 5 - Biofilms, Biomaterials, and Device-Related Infections, in: K. Modjarrad, S. Ebnesajjad (Eds.), Handbook of Polymer Applications in Medicine and Medical Devices, William Andrew Publishing, Oxford, 2013, pp. 77-101.

[9] D. Sharma, L. Misba, A.U. Khan, Antibiotics versus biofilm: an emerging battleground in microbial communities, Antimicrobial Resistance & Infection Control 8(1) (2019) 76.

[10] M.J. Anderson-Glenna, V. Bakkestuen, N.J.W. Clipson, Spatial and temporal variability in epilithic biofilm bacterial communities along an upland river gradient, FEMS Microbiology Ecology 64(3) (2008) 407-418.

[11] T.J. Battin, L.A. Kaplan, J. Denis Newbold, C.M.E. Hansen, Contributions of microbial biofilms to ecosystem processes in stream mesocosms, Nature 426(6965) (2003) 439-442.

[12] Y.-G. Jung, J. Choi, S.-K. Kim, J.-H. Lee, S. Kwon, Embedded biofilm: a new biofilm model based on the embedded growth of bacteria, Applied and Environmental Microbiology (2014) AEM.02311-14.

[13] E. Wright, S. Neethirajan, X. Weng, Microfluidic wound model for studying the behaviors of Pseudomonas aeruginosa in polymicrobial biofilms, Biotechnology and Bioengineering 112(11) (2015) 2351-2359.

[14] T.A. Webster, H.J. Sismaet, I.P.J. Chan, E.D. Goluch, Electrochemically monitoring the antibiotic susceptibility of Pseudomonas aeruginosa biofilms, Analyst 140(21) (2015) 7195-7201.

[15] E. Faure, K. Kwong, D. Nguyen, Pseudomonas aeruginosa in Chronic Lung Infections: How to Adapt Within the Host?, Front Immunol 9 (2018) 2416-2416.

[16] R. Mittal, S. Aggarwal, S. Sharma, S. Chhibber, K. Harjai, Urinary tract infections caused by Pseudomonas aeruginosa: A minireview, Journal of Infection and Public Health 2(3) (2009) 101-111.

[17] S.K. Reza Amin, Alexander Hart, Bekir Yenilmez, Fariba Ghaderinezhad, Sara Katebifar, Michael Messina, Ali Khademhosseini and Savas Tasoglu, 3D-printed microfluidic devices, Biofibracation 8(022001) (2016).

[18] P.A. Suci, M.W. Mittelman, F.P. Yu, G.G. Geesey, Investigation of ciprofloxacin penetration into Pseudomonas aeruginosa biofilms, Antimicrobial Agents and Chemotherapy 38(9) (1994) 2125-2133.

[19] Y.F. Wu, T.Y. Lee, W.T. Liao, H.H. Chuan, N.-C. Cheng, C.M. Cheng, Rapid Detection of Biofilm with Modified Alcian Blue Staining: In-vitro Protocol Improvement and Validation with Clinical Cases, Wound Repair and Regeneration 28 (2020).

[20] M.D. Brazas, R.E.W. Hancock, Ciprofloxacin induction of a susceptibility determinant in Pseudomonas aeruginosa, Antimicrobial agents and chemotherapy 49(8) (2005) 3222-3227.

[21] C. Chen, B.T. Mehl, A.S. Munshi, A.D. Townsend, D.M. Spence, R.S. Martin, 3D-printed microfluidic devices: fabrication, advantages and limitations—a mini review, Analytical Methods 8(31) (2016) 6005-6012.

[22] R.J. Palmer, D.E. Caldwell, A flowcell for the study of plaque removal and regrowth, Journal of Microbiological Methods 24(2) (1995) 171-182.

[23] J. Zhou, D.A. Khodakov, A.V. Ellis, N.H. Voelcker, Surface modification for PDMS-based microfluidic devices, in: Z.E. Rassi (Ed.) Weinheim, 2012, pp. 89-104.

[24] J.S. Teodósio, M. Simões, L.F. Melo, F.J. Mergulhão, Flow cell hydrodynamics and their effects on E. coli biofilm formation under different nutrient conditions and turbulent flow, Biofouling 27(1) (2011) 1-11.

[25] C. Wu, Ji Y. Lim, Gerald G. Fuller, L. Cegelski, Quantitative Analysis of Amyloid-Integrated Biofilms Formed by Uropathogenic Escherichia coli at the Air-Liquid Interface, Biophysical journal 103(3) (2012) 464-471.

[26] P.A. Rühs, L. Böcker, R.F. Inglis, P. Fischer, Studying bacterial hydrophobicity and biofilm formation at liquid–liquid interfaces through interfacial rheology and pendant drop tensiometry, Colloids and surfaces, B, Biointerfaces 117 (2014) 174-184.

15

[27] B. Purevdorj, J.W. Costerton, P. Stoodley, Influence of Hydrodynamics and Cell Signaling on the Structure and Behavior of Pseudomonas aeruginosa Biofilms, Applied and Environmental Microbiology 68(9) (2002) 4457.

[28] R. Kolter, R. Losick, Microbiology: One for all and all for one, Science (Washington) 280(5361) (1998) 226-227.

[29] K.A. Whitehead, J. Verran, The Effect of Substratum Properties on the Survival of Attached Microorganisms on Inert Surfaces, Berlin, Heidelberg: Springer Berlin Heidelberg, Berlin, Heidelberg, 2009.

[30] S. Marti, Biofilm formation at the solid-liquid and air-liquid interfaces by Acinetobacter species, BMC Research Notes (2011).

[31] H. Wang, H. Wu, Z. Song, N. Høiby, Ciprofloxacin shows concentration-dependent killing of Pseudomonas aeruginosa biofilm in vitro, Journal of cystic fibrosis 9 (2010) S41-S41.

[32] Broth Microdilution MIC Test, Clinical Microbiology Procedures Handbook, 3rd Edition, American Society of Microbiology2010.

[33] A. International, ASTM E2799-17, Standard Test Method for Testing Disinfectant Efficacy against Pseudomonas aeruginosa Biofilm using the MBEC Assay, West Conshohocken, PA, , 2017.

[34] H. Ceri, M.E. Olson, C. Stremick, R.R. Read, D. Morck, A. Buret, The Calgary Biofilm Device: New Technology for Rapid Determination of Antibiotic Susceptibilities of Bacterial Biofilms, Journal of Clinical Microbiology 37(6) (1999) 1771.

[35] K.P.e.a. Kim, In situ monitoring of antibiotic susceptibility of bacterial biofilms in a microfluidic device, Lab on a chip 10 (2010) 4.

A

Screw
Plexiglas cover
PDMS chip
Membrane
PDMS chip
Plexiglas cover
Nut

Silicon gaskets

(i) Component of chip

(ii) Assembled device

Top Chamber Inlet
Basal Chamber Outlet
4mm
1mm
Basal Chamber Inlet
Top Chamber Outlet

(iii) Layout and dimension of flow cell

B

3-D printing mold → Pouring the PDMS and curing → Peel off the PDMS replica

C

3-D printing mold → Pouring the silicon and curing → Peel off the silicone gasket

D

Air
Liquid

Liquid
Liquid

	ALI			LLI		
	Detached	**Attached**	**Total**	**Detached**	**Attached**	**Total**
Mean	6.06	7.19	7.24	6.23	6.94	7.15
SD	0.99	0.87	0.87	0.98	0.95	0.91
SEM	0.24	0.20	0.20	0.23	0.22	0.22

Detached = cells washed off by rinsing; attached = cells remaining on the membrane after washing and detached from the membrane after sonication; total = the sum of detached and attached. The mean value, standard deviation (SD) and standard error of mean results (SEM) are expressed as Log(CFU/mL) of n=18.

19